

Effective charge saturation in colloidal suspensions

Lydéric Bocquet¹, Emmanuel Trizac², and Miguel Aubouy³

¹ *Laboratoire de Physique de l'E.N.S. de Lyon, UMR CNRS 5672, 46 Allée d'Italie, 69364 Lyon Cedex, France*

² *Laboratoire de Physique Théorique, UMR CNRS 8627, Bâtiment 210, Université Paris-Sud, 91405 Orsay Cedex, France*

³ *S.I.3M., D.R.F.M.C., CEA-DSM Grenoble, 17 rue des Martyrs, 38054 Grenoble Cedex 9, France*

(March 22, 2022)

Because micro-ions accumulate around highly charged colloidal particles in electrolyte solutions, the relevant parameter to compute their interactions is not the bare charge, but an effective (or renormalized) quantity, whose value is sensitive to the geometry of the colloid, the temperature or the presence of added-salt. This non-linear screening effect is a central feature in the field of colloidal suspensions or polyelectrolyte solutions. We propose a simple method to predict effective charges of highly charged macro-ions, that is reliable for mono-valent electrolytes (and counter-ions) in the colloidal limit (large size compared to both screening length and Bjerrum length). Taking reference to the non linear Poisson-Boltzmann theory, the method is successfully tested against the geometry of the macro-ions, the possible confinement in a Wigner-Seitz cell, and the presence of added salt. Moreover, our results are corroborated by various experimental measures reported in the literature. This approach provides a useful route to incorporate the non-linear effects of charge renormalization within a linear theory for systems where electrostatic interactions play an important role.

I. INTRODUCTION

When a solid-like object, say a colloidal particle (polyion), which carries a large number of ionisable groups at the surface is immersed in a polarizable medium (with a dielectric constant ϵ , say water), the ionisable groups dissociate, leaving counter-ions in the solutions and opposite charges at the surface. The interactions between the charged colloids, which determine the phase and structural behaviour of the suspension, is mediated by the presence of micro-ions clouds. The complete description of the system is thus a formidable task in general. However in view of the large asymmetry of size and charge between macro- and micro- ions, one expects to be able to integrate out the micro-ions degrees of freedom, and obtain an effective description involving macro-ions only. In the pioneering work of Derjaguin, Landau, Verwey and Overbeek [1], micro-ions clouds are treated at the mean-field Poisson-Boltzmann (PB) level, yielding the foundations of the prominent DLVO theory for the stability of lyophobic colloids. An important prediction of the theory is the effective interaction pair potential between two spherical colloids of radii a in a solvent which, within a linearization approximation, takes the Yukawa or Debye-Hückel (DH) form:

$$v(r) = \frac{Z^2 e^2}{4\pi\epsilon} \left(\frac{\exp[\kappa a]}{1 + \kappa a} \right)^2 \frac{\exp(-\kappa r)}{r}, \quad (1)$$

where Z is the charge of the object in units of the elementary charge e and κ denotes the inverse Debye screening length. The latter is defined in terms of the micro-ions densities $\{\rho_\alpha\}$ (with valences $\{z_\alpha\}$) as: $\kappa^2 = 4\pi\ell_B \sum_\alpha \rho_\alpha z_\alpha^2$. The Bjerrum length ℓ_B is defined as $\ell_B = e^2/(4\pi\epsilon k_B T)$, where ϵ is the permittivity of the solvent considered as a dielectric continuum: $\ell_B = 7 \text{ \AA}$ for water at room temperature.

However, this approach becomes inadequate to describe highly charged objects for which the electrostatic energy of a micro-ion near the colloid surface largely exceeds $k_B T$, the thermal energy, because the linearization of the PB equations is *a priori* not justified. In this case however, the electrostatic potential in exact [2,3] or mean-field [4,5] theories still takes the Debye-Hückel like form far from the charged bodies, provided that the bare charge Z is replaced by an effective or renormalized quantity Z_{eff} . The micro-ions which suffer a high electrostatic coupling with the colloid accordingly accumulate in its immediate vicinity so that the decorated object, colloid *plus* captive counter-ions, may be considered as a single entity which carries an effective charge Z_{eff} , much lower (in absolute value) than the structural one. Within the prominent mean-field PB theory [6] –often quite successful despite of its limitations–, Z and Z_{eff} coincide for low values of the structural charge, but Z_{eff} eventually reaches a saturation value $Z_{\text{eff}}^{\text{sat}}$ independent of Z when the bare charge increases [5,7]. Arguably, the difference $Z - Z_{\text{eff}}$ is identified with the amount of counter-ions “captured” or “condensed” [8] onto the macro-ion.

A reminiscent effect has been recognized in the physics of polyelectrolytes under the name of Manning-Oosawa condensation. Here, the object is an infinitely long and thin rod bearing λ charges per unit length. At infinite

dilution and in the absence of salt, it can be shown at the PB level that the polyelectrolyte is electrostatically equivalent to a rod carrying λ_{equiv} charge per unit length, where the equivalent charge density saturates to a critical value $\lambda_{\text{equiv}} = 1/\ell_B$ when λ increases [9–11]. In general however, PB theory can be solved analytically in very few geometries only and the difficulty remains to predict Z_{eff} for a given colloidal system [4,5,7,12,13]. In the absence of a general analytical framework for the computation of the effective charge, this quantity is often considered as an adjustable parameter to fit experimental data [14,15].

The aim of the present paper is to propose a method that allows to compute effective charges comparing favorably with PB in the saturation regime, provided the size a of the charged macro-ion is much larger than Bjerrum length ℓ_B and screening length κ^{-1} . In the infinite dilution limit, we define the effective charges from the large distance behaviour of the electrostatic potential created by the (isolated) macro-ion [16]. While other definitions have been put forward [4,17–19] this choice is relevant in view of computing a macro-ion pair potential at large distances, in the spirit of the DLVO approach [20]. It moreover avoids the ambiguity of introducing a cutoff region in space which interior containing the colloid would exactly enclose a total charge equal to the effective one. At leading order in curvature $(\kappa a)^{-1}$, our method easily provides effective charges at saturation close to their counterparts obtained in PB theory. In the situation of finite colloid concentration where it is no longer obvious to extract an effective charge from the large distance behaviour of the electrostatic potential computed within a non-linear theory, we follow the proposition put forward by Alexander *et al.* [5] introducing a Wigner-Seitz cell. In this situation, we generalize our original method into a prescription that we successfully test in various geometries, for different thermodynamic conditions (isolated systems or in contact with a salt reservoir).

The paper is organized as follows. We first recall the basic framework of PB theory in section II. We then examine in some details the simple case of a spherical polyion in the infinite dilution limit (section III). This example allows us to devise a general method to compute the effective charge for arbitrary colloidal systems. The situation of finite density of colloids is then examined introducing Wigner-Seitz cells. The salt free case is developed in section IV, while the situation of finite ionic force is explicit in section V. We finally confront the results obtained within our prescription with experimental or simulation data in various geometries in section VI. We discuss the general validity of our mean-field treatment relying on PB approximation in section VII and conclusions are drawn in section VIII. The preliminary results of this study have been published elsewhere [21].

II. GENERAL FRAMEWORK: POISSON-BOLTZMANN THEORY

Poisson-Boltzmann theory provides a mean field description of the micro-ions clouds in the presence of the polyions, acting as an external potential. The key approximation in the approach is the neglect of (micro-)ionic correlations. The size of the micro-ions with density ρ is neglected as well and the chemical potential reduces to its ideal contribution $\mu = k_B T \ln(\rho \Lambda^3)$, where Λ is an irrelevant length scale. Without loss of generality, the macro-ions are supposed to be positively charged.

At equilibrium the *electro-chemical* potential of the micro-ions is uniform over the system. Introducing the reduced electrostatic potential $\phi = eV/k_B T$, the equilibrium condition for micro-ions thus reads at the mean field level

$$\ln(\rho^\pm \Lambda^3) \pm \phi = \ln(\rho_0 \Lambda^3) \quad (2)$$

where $\{\rho^-, \rho^+\}$ are the density fields of the charged micro-species (counter-ions and co-ions), which we assume for simplicity mono-valent. The constant ρ_0 will be specified hereafter. We restrict here to mono-valent micro-ions (both counter-ions and salt). For higher valences, the reliability of PB deteriorates (see section VII). The equilibrium condition, Eq. (2), is closed by Poisson's equation for the electrostatic potential

$$\nabla^2 \phi = -4\pi \ell_B (\rho^+ - \rho^-). \quad (3)$$

The gradient of equation (2) expresses the condition of mechanical equilibrium for the fluid of micro-ions [22]. At this level, one has to separate between the no-salt and finite ionic strength cases.

- *No-Salt Case* Only the released (here negative) counter-ions are present in the system. The PB equation for the reduced potential thus reads

$$\nabla^2 \phi = \kappa^2 e^\phi \quad (4)$$

where the screening constant κ is defined as $\kappa^2 = 4\pi \ell_B \rho_0$, with ρ_0 the constant introduced in Eq. (2). The latter is fixed by the electroneutrality condition, which imposes

$$\int_{\mathcal{V}} d\mathbf{r} \rho^-(\mathbf{r}) = -ZeN_c \quad (5)$$

with N_c the number of (identical) macro-ions, of charge Ze , contained in the volume \mathcal{V} . The quantity ρ_0 is a Lagrange multiplier associated with the electroneutrality condition and has no specific physical meaning; it is modified by a shift of potential, which can be chosen at our convenience to fix ϕ at a given point in the solution.

- *Finite Ionic strength situation* In the finite ionic strength case, salt is added to the solution, so that both co- and counter- ions are present in the system. In the following we shall work in the semi-grand ensemble, where the { colloids+micro-ions } system is put in contact with a reservoir fixing the chemical potential of the micro-ions μ_0 . In this case ρ_0 in Eq. (2) is the concentration of salt in the reservoir (where ϕ is conveniently chosen to vanish), so that $\mu_0 = k_B T \ln(\rho_0 \Lambda^3)$. Since we are considering mono-valent micro-ions ρ_0 coincides with the ionic strength of the reservoir which is generally defined as $I_0 = n_\alpha^{-1} \sum_\alpha z_\alpha^2 \rho_\alpha^0$ for a number n_α of micro-ions species with valences z_α and reservoir densities ρ_α^0 . This results in the PB equation for the reduced potential ϕ

$$\nabla^2 \phi = \kappa^2 \sinh \phi \quad (6)$$

where the screening factor κ is now defined in terms of the micro-ion concentration in the reservoir $\kappa^2 = 8\pi\ell_B I_0 \equiv \kappa_{\text{res}}^2$.

In addition to these two situations, we shall also consider the case of infinite dilution where an isolated macro-ion is immersed in an electrolyte of given bulk salt concentration I_0 which thus plays the role of a reservoir.

PB equations, (4) or (6), are supplemented by a set of boundary conditions on the colloids, expressing the relationship between the local electric field and the *bare* surface charges of the colloidal particles, σe . This gives the boundary condition for ϕ at the surface of the colloid in the form

$$(\nabla \phi) \cdot \hat{\mathbf{n}} = -4\pi\ell_B \sigma, \quad (7)$$

where $\hat{\mathbf{n}}$ denotes a unit vector normal to the colloid's surface. Except in simple isotropic geometries [23], the analytical solution of PB theory is not known.

III. INFINITE DILUTION LIMIT: ASYMPTOTIC MATCHING FOR THE EFFECTIVE CHARGE

In this section, after recalling a few results on the planar case, we explicit our method on the particular example of spheroids. We then generalize it to an arbitrary colloidal object and consider the case of charged rods as an application. We work in the infinite dilution limit, and therefore, we reject the external boundaries of the system at infinity.

A. Planar Case

In the case of the planar geometry, the non linear PB equation can be analytically solved. The detailed solution is given in appendix A. The important result however is that far from the charged plane, the solution of the PB equation reduces to that of the LPB equation :

$$\phi_{\text{PB}}(z) \simeq \phi_S e^{-\kappa z} \quad (8)$$

The *apparent* potential ϕ_S is equal to $\phi_S = 4$ in the limit of high bare charge of the plane.

In this limit, the fixed charge boundary condition is therefore replaced on the plane by an effective *fixed surface potential* boundary condition $\phi_{\text{LPB}}(z=0) = \phi_S = 4$. The effective charge density (in the saturation-high bare charge- limit) is then computed using Gauss theorem at the surface, yielding

$$\sigma_{\text{eff}}^{\text{sat}} = \frac{\kappa}{\pi\ell_B}. \quad (9)$$

B. Charged spheres

Let us now consider a highly charged isolated sphere (bare charge Ze , radius a) immersed in a symmetric 1:1 electrolyte of bulk ionic strength I_0 . Within PB theory, the dimensionless electrostatic potential obeys equation (6). Suppose we know the exact solution $\phi_{\text{PB}}(r)$ (in spherical coordinates with the origin at the center of the sphere), and the bare charge Z is large enough so that the reduced electrostatic potential at contact, $\phi_{\text{PB}}(a)$, is (much) larger than 1. Then, we can divide the space surrounding the polyion into two sub-regions: a non-linear region (close to the particle's boundary) where $\phi_{\text{PB}}(r) > 1$, and a linear region where $\phi_{\text{PB}}(r) < 1$ (the potential vanishes at infinity). The surface delimiting these two regions is a sphere of radius r^* such that $\phi_{\text{PB}}(r^*) \simeq 1$.

Far from colloid, the complicated non-linear effects have died out to a substantial degree, and the solution also obeys the linearized Poisson-Boltzmann (LPB) equation $\nabla^2 \phi = \kappa^2 \phi$, and therefore takes the Yukawa form

$$\phi_{\text{LPB}}(r) = \frac{Z_{\text{eff}}}{(1 + \kappa a)} \ell_B \frac{e^{-\kappa(r-a)}}{r}. \quad (10)$$

The effective charge Z_{eff} is defined here without ambiguity from the far field behaviour of $\phi_{\text{PB}}(r)$:

$$\lim_{r \rightarrow \infty} \phi_{\text{LPB}}(r)/\phi_{\text{PB}}(r) = 1. \quad (11)$$

In practice, ϕ_{LPB} and ϕ_{PB} coincide in the linear region ($r \gtrsim r^*$), so that $\phi_{\text{LPB}}(r^*) \simeq 1$ (i.e. is a quantity of order one).

When $a \gg \kappa^{-1}$, the non-linear effects are confined to the immediate vicinity of the macro-ion, with an extension κ^{-1} . We therefore have $r^*/a \simeq 1$ and as a consequence, $\phi_{\text{LPB}}(r = a) \simeq \phi_{\text{LPB}}(r^*) \simeq 1$. We thus obtain the effective boundary condition that ϕ_{LPB} is a quantity \mathcal{C} of order one for $r = a$; from Eq. (10) this means that $Z_{\text{eff}}^{\text{sat}} = \mathcal{C}a(1 + \kappa a)/\ell_B$. This simple argument provides the non trivial dependence of the effective charge at saturation upon physico-chemical parameters; it applies in the saturation regime of PB theory where $Z_{\text{eff}} = Z_{\text{eff}}^{\text{sat}}$ and assumes that the bare charge Z is high enough so that the non-linear region exists. In order to determine the constant \mathcal{C} , we may consider the planar limit $a \rightarrow \infty$ where the analytical solution of PB theory is known (see above and appendix A): the surface charge density $Z_{\text{eff}}^{\text{sat}}/(4\pi a^2)$ should coincide with that of a charged plane $\kappa/(\pi\ell_B)$, Eq. (9). This imposes that $\mathcal{C} = 4$ and going back to the charge:

$$Z_{\text{eff}}^{\text{sat}} = \frac{4a}{\ell_B} (1 + \kappa a). \quad (12)$$

In de-ionized solutions, this argument leads to the scaling $Z_{\text{eff}}^{\text{sat}} \propto a/\ell_B$, which has been recently tested for various latex colloids [24].

The physical argument leading to (12) may be rationalized as follows. The situation of large κa corresponds to a low curvature limit where the solution of Eq. (6) may be approximated by the solution of the planar problem in the region where curvature effects may be neglected: the latter corresponds to a region $a < r < a + \delta a$, with $\delta a \sim a$. It is crucial to note that $r^* < a + \delta a$ since, as mentioned above, the extension of the region where the non linear effects are important (defining r^*) has an extension of order κ^{-1} , smaller than $\delta a \sim a$ in the limit of large κa . As a consequence, in the region $r^* < r < a + \delta a$, the solution of the LPB equation, Eq. (10), may be matched to the asymptotic expression of the *planar* solution, given in Eq. (8) (using $r \sim a$ and $z \simeq r - a$). The expression (12) is therefore recovered, showing again that at the linearized level, the apparent potential is $\phi_{\text{LPB}}(a) = 4$ in the saturation limit.

Eq. (12) provides by construction the correct large κa behaviour of $Z_{\text{eff}}^{\text{sat}}$, and becomes exact (compared to PB) in the planar limit. We will show below that it remains fairly accurate down to κa of order 1. A similar expression may be found in [25,26], but the generality of the underlying method does not seem to have been recognized. This result is supported by the work of Oshima *et al.* [27] which proposes an approximation scheme of the non-linear PB equations for spheres in infinite dilution, for large κa . In particular these authors obtain an analytical approximation for the apparent potential at the colloid surface, which reads in the saturation regime:

$$\phi_S^{\text{Osh}} = 8 \frac{1 + \kappa a}{1 + 2\kappa a}. \quad (13)$$

Supplemented with expression (10), this leads to the improved effective charge

$$Z_{\text{eff}}^{\text{sat}} = \frac{8a}{\ell_B} \frac{(1 + \kappa a)^2}{1 + 2\kappa a}. \quad (14)$$

In the limit of large κa where $\phi_S \rightarrow 4$, both Eqs. (12) and (14) have the same behaviour.

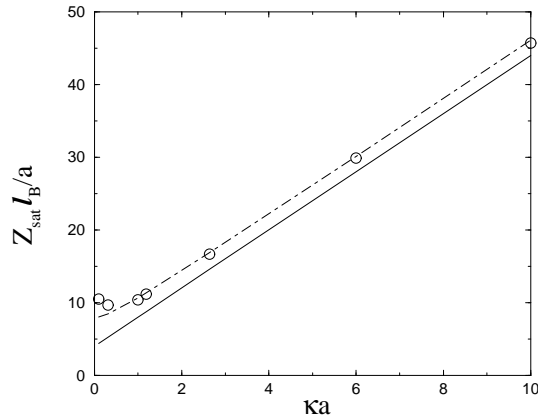


FIG. 1. Effective charge in the saturation regime $Z_{\text{eff}}^{\text{sat}} \ell_B / a$ as a function of κa for spheres in the infinite dilution limit with added salt. The symbols (open circle) are the “exact” solution estimated from the large distance behaviour of the electrostatic potential solution of the full non-linear PB equation. The continuous (resp. dashed) line is Z_{sat} found with Eq. (12) [resp. Eq. (14)].

In order to test the validity of these results, we have numerically solved the full non-linear PB equation, Eq. (6) and computed the effective charge from the electrostatic potential at large distances, *i.e.* the value required to match ϕ_{LPB} to the far field ϕ_{PB} obtained numerically. For each value of κa , we make sure to consider large enough bare charges in order to probe the saturation regime of Z_{eff} . Figure 1 compares the numerical PB saturation value of the effective charge to the prediction of our approach, Eq. (12), and to that obtained using the results of Oshima *et al.*, Eq. (14). We see that Eq. (14) provides an accurate estimate for $Z_{\text{eff}}^{\text{sat}}$ as a function of κa , for $\kappa a \gtrsim 1$. Working at the level of our approach only, Eq. (12) still yields a reasonable estimate for $Z_{\text{eff}}^{\text{sat}}(\kappa a)$, specially for high values of the parameter κa . In the limit of small κa , both expressions (12) and (14) differ notably from the PB saturation charge which diverges, as shown by Ramanathan [28], as:

$$Z_{\text{eff}}^{\text{sat}} \sim \frac{a}{\ell_B} \{-2 \ln(\kappa a) + 2 \ln[-\ln(\kappa a)] + 4 \ln 2\} \quad \text{for } \kappa a \rightarrow 0. \quad (15)$$

At this point, it is instructive to briefly reconsider the work of Squires and Brenner [29] who demonstrated that the attractive interactions between like-charged colloidal spheres near a wall could be accounted for by a non-equilibrium hydrodynamic effect (see also [22]). In their analysis, they used an ad hoc value of 0.4 for the ratio $\sigma_{\text{glass}}/\sigma_{\text{sphere}}$ of surface charge densities of planar and spherical polyions, in order to capture the one-wall experiment of Larsen and Grier [30]. This was the only free parameter in their approach. From Eqs. (A6) and (14) for the saturation values, we easily obtain

$$\frac{\sigma_{\text{glass}}}{\sigma_{\text{sphere}}} = \frac{\kappa a(1 + 2\kappa a)}{2(1 + \kappa a)^2}. \quad (16)$$

In the experiment of [30], we have $\kappa a \simeq 1.2$ [larger than 1, so that (14) is reasonably accurate], and we obtain $\sigma_{\text{glass}}/\sigma_{\text{sphere}} \simeq 0.42$: it is thus possible to justify the choice made in [29] assuming that both the confining wall and the pair of colloids are charged enough to sit in the saturation regime. In this respect, knowledge of their bare charges is unnecessary.

C. Arbitrary colloidal object

Generalizing this analysis for an arbitrary colloidal object (of typical size a), we propose the following method to estimate the effective charge in the limit of large values of κa :

1. Solve the LPB equation for the geometry under consideration
2. Define the saturation value, $Z_{\text{eff}}^{\text{sat}}$, such that the linear reduced potential at contact is a constant, \mathcal{C} , of order unity

$$|\phi_S - \phi_{\text{bulk}}| = \mathcal{C}, \quad (17)$$

where the asymptotic matching with the planar case yields $\mathcal{C} = 4$.

3. If one is interested in the effective charge for arbitrary and possibly small bare charges, a crude approximation follows from

$$\begin{aligned} Z_{\text{eff}} &= Z & Z &\ll Z_{\text{eff}}^{\text{sat}} \\ Z_{\text{eff}} &= Z_{\text{eff}}^{\text{sat}} & Z &\gg Z_{\text{eff}}^{\text{sat}}. \end{aligned} \quad (18)$$

Our approach has several advantages. First, we do not need to solve the full non-linear PB equations to obtain the effective charge. Second, the proposed method provides an analytical prediction for $Z_{\text{eff}}^{\text{sat}}$. Third, our approach is easily adapted to other macro-ion geometries or finite dilutions, unlike that of Ref. [27] (even if these authors could find an equivalent of expression (13) for cylinders, see below).

In the following, we will mainly focus on the high bare charge limit of the colloids where the effective charge reaches a saturation plateau, $Z_{\text{eff}}^{\text{sat}}$. In order to simplify notations, we will denote this saturation value Z_{sat} .

D. Rod-like macro-ions

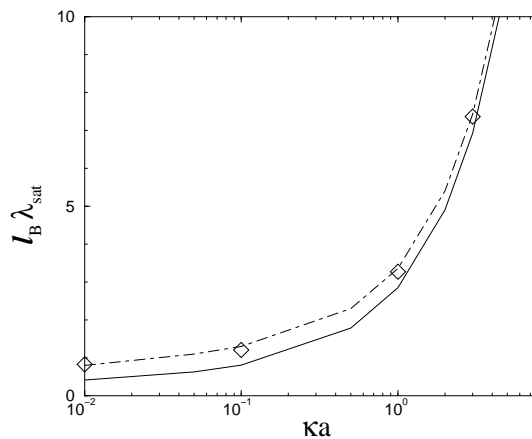


FIG. 2. Effective line charge density, $\ell_B \lambda_{\text{sat}}$, versus κa (the reduced Debye-Hückel constant) for cylinders in the infinite dilution limit with added salt. The symbols (open diamonds) are computed from the large distance behaviour of the electrostatic potential solution of the full non-linear PB equation, solved numerically. The continuous (resp. dashed) line is our estimate for $\ell_B \lambda_{\text{sat}}$, Eq. (21) [resp. the improved estimate, Eq. (23)].

Now the object is an infinitely long cylinder (radius a , bare line charge density λe). The solution of linear PB equation is (in cylindrical coordinates where r is the distance to the axis)

$$\phi(r) = 2\lambda\ell_B \frac{1}{\kappa a} \frac{K_0(\kappa r)}{K_1(\kappa a)}, \quad (19)$$

where K_0 and K_1 are (respectively) the zero and first order modified Bessel functions of the second kind. Hence the apparent potential is

$$\phi_S = 2\lambda\ell_B \frac{1}{\kappa a} \frac{K_0(\kappa a)}{K_1(\kappa a)} \quad (20)$$

Setting $\phi_S = \mathcal{C} = 4$ yields our estimate for the effective line charge density at saturation

$$\lambda_{\text{sat}} = \frac{2\kappa a}{\ell_B} \frac{K_1(\kappa a)}{K_0(\kappa a)}. \quad (21)$$

In the limit of large values of the bare line charge density λ , Oshima *et al.* obtained an approximate expression for the apparent potential in the saturation regime (based on an approximation scheme for the PB equation, see Appendix A of Ref. [27]):

$$\phi_S^{\text{Osh}} = 8 \frac{K_1(\kappa a)}{[K_0(\kappa a) + K_1(\kappa a)]} \quad (22)$$

As expected, we note that $\phi_S^{\text{Osh}} \rightarrow 4$ in the limit $\kappa a \gg 1$. However, from Eq. (22), we deduce an improved estimate of λ_{sat}

$$\lambda_{\text{sat}} = \frac{4\kappa a}{\ell_B} \frac{K_1(\kappa a)}{K_0(\kappa a)} \frac{K_1(\kappa a)}{[K_0(\kappa a) + K_1(\kappa a)]}. \quad (23)$$

In Fig. 2, we display $\ell_B \lambda_{\text{sat}}$ [estimated either with Eq. (21) or Eq. (23)] as a function of κa , together with the “exact” value of $\ell_B \lambda_{\text{sat}}$ found by solving the full non-linear PB equation for high bare charges in the saturation regime. Note that the plot is in log-linear scale, in order to emphasize the small κa region where our method is not *a priori* expected to work. Surprisingly, the agreement between the numerical result of the full PB equation and (23) is satisfactory down to very low values of κa , $\kappa a \sim 10^{-2}$, although the two quantities have a different asymptotic behaviour: the exact $\ell_B \lambda_{\text{sat}}$ is finite when $\kappa a \rightarrow 0$ ($\ell_B \lambda_{\text{sat}} = 2/\pi$ from ref. [31], see next paragraph), whereas both estimate Eq. (21) and (23) vanish, although extremely slowly (as $-1/\log(\kappa a)$).

Importantly, $\kappa a \rightarrow 0$ is the asymptotic regime where the celebrated Manning limiting law [11,32] happens to be exact, and the condensation criterion holds. In this limit, above the condensation threshold, the electrostatic potential solution of the full non-linear PB equation is indistinguishable from that of a cylinder carrying a line charge density $\lambda_{\text{equiv}} = 1/\ell_B$ [11]. The two quantities λ_{equiv} and λ_{sat} may be coined as “effective charges”, but we maintain our initial definition of the effective charge from the far field potential solution of the non-linear PB equation. In this respect, $\lambda_{\text{equiv}} \neq \lambda_{\text{sat}}$, (as already discussed in the Appendix of reference [11]). This is because one expects a remnant non-linear screening of λ_{equiv} , so that $\lambda_{\text{sat}} < \lambda_{\text{equiv}} = 1/\ell_B$. The limiting situation $\kappa a \rightarrow 0$ has been solved recently within Poisson-Boltzmann theory, using exact results from the theory of integrable systems [31]. The corresponding solution illustrates our point. This seminal work allows to compute explicitly the effective charge, which reads

$$\lim_{\kappa a \rightarrow 0} \lambda_{\text{eff}} = \frac{2}{\pi \ell_B} \sin\left(\frac{\pi}{2} \lambda \ell_B\right). \quad (24)$$

Accordingly, when λ exceeds the Manning threshold $1/\ell_B$, the effective charge saturates to a value

$$\lambda_{\text{sat}} = \frac{2}{\pi \ell_B} \cong \frac{0.6366}{\ell_B} < \lambda_{\text{equiv}} = \frac{1}{\ell_B}. \quad (25)$$

It is noteworthy that the limit $2/(\pi \ell_B)$ (compatible with the numerical results reported by Fixman, see for example Fig. 1 of ref. [32]) is reached extremely slowly as κa is decreased, in practice for $\kappa a < 10^{-6}$. For example, for $\kappa a = 10^{-2}$, the numerical solution of the PB equation yields $\lambda_{\text{sat}} \cong 0.81/\ell_B$, hence a value 30% larger than the asymptotic limit.

IV. EFFECTIVE CHARGE AT FINITE CONCENTRATION. THE NO-SALT CASE

The situation of finite density of colloids does not allow to define an effective charge from the far field of a single body potential, as done in section III. Here, we rely on the proposition put forward by Alexander *et al.* to define an effective charge [5]. We recall here the main points of this PB cell approach. First, the procedure makes use of the concept of Wigner-Seitz (WS) cells: the influence of the other colloids is accounted for by confining the macro-ion into a cell, with global electroneutrality [33–36]. The size of the cell, R_{WS} is computed from the density of colloids, while its geometry is chosen as to mimic the spatial structure of the colloids in the solution. Second, the “effective” potential solution of the linearized PB equation is such that the linear and non-linear solutions match up to the second derivative at the boundaries of the WS cell (hence they match up to at least the third derivative because of electroneutrality in “isotropic” –spherical or cylindrical– cells). Note that in the original paper of Alexander *et al.* the procedure was introduced to obtain the effective charge from the *numerical* solution of the non linear PB equation. But in the present work we shall use the approach to get effective charges at the LPB level together with our prescription. Such a route has proven successful for mono-valent micro-ions, see e.g. [37–39], and it has been shown recently that similar ideas could be employed to describe discrete solvent effects (again for mono-valent micro-ions [40]).

In this section, we generalize the analysis proposed in section III C to find a prescription suitable to treat the case of finite concentration of colloids. We eventually compare our results to those obtained following ref. [5], for planar, cylindrical and spherical geometries.

A. Generalized prescription and planar test case

In the infinite dilution case, the reference potential is the bulk one ϕ_{bulk} . The natural generalization of this choice for the finite concentration case consists in replacing in Eq. (17) ϕ_{bulk} by ϕ_{Σ} the reduced electrostatic potential at the boundary of the WS cell. Hence, we propose

$$|\phi_S - \phi_{\Sigma}| = \mathcal{C}. \quad (26)$$

If added salt was present in the suspension (see section V), we should recover Eq. (17) from Eq. (26) in the infinite dilution limit where R_{WS} goes to infinity. We consequently expect the value $\mathcal{C} = 4$ to be relevant for the situation of finite density of colloids with added salt. Searching for a unified description, we also test the possible validity of the choice $\mathcal{C} = 4$ in the no salt situation. It is therefore instructive, as an illustration of the method and benchmark, to analyze the simple case of a charged plane confined in a WS cell, without added electrolyte. As recalled in Appendix B, the analytical solution of the non linear PB equation is known in such a geometry when counter-ions are the only micro-ions present, which allows to check the validity of our assumptions in the limiting case of finite concentration. Below, we compare these “exact” results to the predictions of our prescription.

The exact apparent potential, ϕ_S is obtained using Eq. (B5) at $x = 0$ for the plane: $\phi_S = \cosh(K_{\text{LPB}}h) - 1$. Our prescription imposes $\phi_S = 4$, yielding $K_{\text{LPB}}h = \text{ArcCosh}(5)$. The effective charge is obtained from Gauss theorem at the surface, *i.e.* Eq. (B6) with σ replaced by σ_{eff} . This leads to the final result of our prescription $\sigma_{\text{sat}} = \sqrt{6}\text{ArcCosh}(5)\sigma_c \cong 5.6\sigma_c$ (where $\sigma_c = 1/\pi l_B h$), which should be compared to the exact result $\sigma_{\text{sat}} \simeq 5.06\sigma_c$ [see Eq. (B12) in appendix B]. First it is striking to note that our prescription predicts the correct functional dependence of the effective charge in terms of the parameters of the system. Moreover the numerical prefactor in front of σ_c is only within 10% of the “exact” value obtained in Eq. (B12), which is quite a satisfactory agreement.

However certainly the most interesting feature which comes out from the previous results is the fact that the apparent potential at contact, ϕ_S , obtained within the analytical resolution of the PB equation, does saturate to a constant value $\phi_S \simeq 3.66$ in the limit of very large bare charges: this value is very close to the value we prescribe, $\phi_S = 4$! This is a non trivial point, since the physical conditions in the present case are very different from the isolated plane case (previous section). We conclude that the analytic results available for a confined one-dimensional electric double-layer support our prescription. For a more refined analysis of the electrostatics of counter-ions between planar charged walls, going beyond PB, we refer to the work of Netz *et al.* [41].

In the remaining of this section, we further test our prescription against results for spherical and cylindrical macro-ions.

B. Spheroids

Here, the object is a charged spherical colloid (bare charge Ze , radius a) confined with its counter-ions in a concentric WS sphere (radius R_{WS}). The packing fraction is defined as $\eta = (a/R_{WS})^3$. PB equation is again linearized around the boundary of the WS cell, yielding Eq. (B4) which we recall here:

$$\nabla^2 \phi = K_{\text{LPB}}^2 (\phi + 1). \quad (27)$$

As for the planar case, the boundary conditions are $\nabla \phi(R_{WS}) = 0$ (electroneutrality), $\phi_{\text{LPB}}(R) = 0$ (because we impose by commodity the potential to vanish at the WS cell, see Appendix B). The solution ϕ_{LPB} thus reads:

$$\phi_{\text{LPB}}(r) = -1 + f_+ \frac{e^{K_{\text{LPB}}r}}{r} + f_- \frac{e^{-K_{\text{LPB}}r}}{r} \quad (28)$$

with

$$f_{\pm} = \frac{K_{\text{LPB}}R_{WS} \pm 1}{2K_{\text{LPB}}} \exp(\mp K_{\text{LPB}}R_{WS}). \quad (29)$$

The charge Z_{eff} of the colloid is obtained from the spatial derivative of ϕ_{LPB} at the colloid surface:

$$Z_{\text{eff}} = \frac{a}{\ell_B} \frac{1}{K_{\text{LPB}}a} \left\{ (1 - K_{\text{LPB}}^2 a R_{WS}) \sinh[K_{\text{LPB}}(R_{WS} - a)] - K_{\text{LPB}}(R_{WS} - a) \cosh[K_{\text{LPB}}(R_{WS} - a)] \right\}. \quad (30)$$

At this level the screening constant K_{LPB} is still unknown: it is fixed by our prescription which imposes the apparent potential of the colloid, such that $\phi_{\text{LPB}}(r=a) = \mathcal{C} = 4$ with $\phi_{\text{LPB}}(r)$ given in Eq. (28). The effective charge, Z_{sat} , is eventually computed using Eq. (30). On the other hand K_{PB} is defined from the PB counter-ion density at WS boundary $\rho^-(WS)$:

$$K_{\text{PB}}^2 = 4\pi\ell_B\rho^-(WS). \quad (31)$$

The equation for K_{LPB} , $\phi_{\text{LPB}}(r=a) = 4$, is solved numerically using a simple Newton procedure. Fig. 3 displays the corresponding Z_{sat} as a function of η together with the effective charge (again at saturation) found by solving *numerically* the full non linear PB equation, together with Alexander's procedure. We recall that this procedure defines the effective charge entering LPB equation such that the solution of PB and LPB equations match up to the second derivative at the WS boundary. We emphasize that once PB equation has been solved numerically, no further numerical fitting procedure is required to match ϕ_{LPB} to ϕ_{PB} and compute the effective charge: the counter-ion density at WS boundary $\rho^-(WS)$ is known and K_{PB} follows from Eq. (31). Replacing K_{LPB} with this value in Eq. (30) then gives the "Alexander" Z_{eff} (a similar remark holds with added salt, see below). We see again that our prescription works reasonably well.

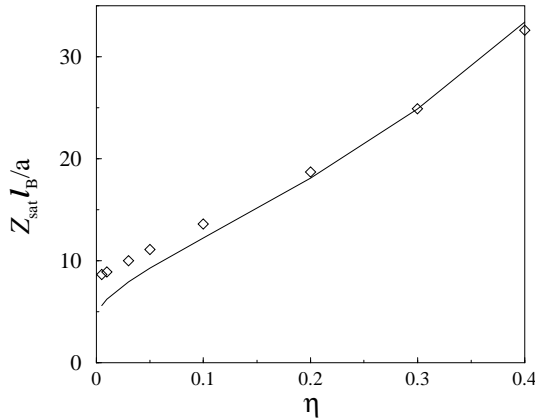


FIG. 3. Effective charge at saturation versus packing fraction for spherical polyions without added salt. The symbols (open diamonds) represent the effective charge found by solving numerically the non linear PB theory supplemented with Alexander's procedure [5]. The continuous line is Z_{sat} within our prescription.

C. Cylinders

Here we apply the previous procedure to an infinite cylinder (radius a , bare charge per unit length λe) enclosed in a WS cylinder (same axis, radius R_{WS}). We define the packing fraction as $\eta = (a/R_{WS})^2$. This case is particularly interesting since the solution of the PB equation in the no-salt case is known from the work of Fuoss *et al.* and Alfrey *et al.* [10]. This therefore provides another critical test of our prescription. We note that a similar approach has been followed by H. Löwen [38].

The calculation follows the same lines as for the previous spherical case. The solution of LPB equation (27) in the two dimensional case, with the usual boundary conditions and the choice $\phi_{\text{LPB}}(R_{WS}) = 0$ reads:

$$\phi_{\text{LPB}}(\rho) = -1 + K_{\text{LPB}}R_{WS} \left\{ I_1(K_{\text{LPB}}R_{WS})K_0(K_{\text{LPB}}\rho) + K_1(K_{\text{LPB}}R_{WS})I_0(K_{\text{LPB}}\rho) \right\}, \quad (32)$$

where use was made of the identity $x[I_0(x)K_1(x) + I_1(x)K_0(x)] = 1$. From the spatial derivative of ϕ_{LPB} at $r = a$ we deduce the effective line charge density λ_{eff} :

$$\lambda_{\text{eff}}\ell_B = \frac{1}{2} K_{\text{LPB}}^2 a R_{WS} \left\{ I_1(K_{\text{LPB}}R_{WS})K_1(K_{\text{LPB}}a) - I_1(K_{\text{LPB}}a)K_1(K_{\text{LPB}}R_{WS}) \right\}. \quad (33)$$

If the above expression is evaluated replacing K_{LPB} by the exact K_{PB} following from (31) once the non-linear problem has been numerically solved, we obtain the original Alexander value (not necessarily at saturation, and

without having to implement in practice a numerical fitting procedure). On the other hand, as in the spherical case, the screening constant K_{LPB} at saturation is obtained (approximately) by imposing the potential at the polyion's surface: $\phi_{\text{LPB}}(a) = \mathcal{C} = 4$ in the previous equation for ϕ_{LPB} . Evaluation of Eq. (33) then gives the saturation value λ_{sat} .

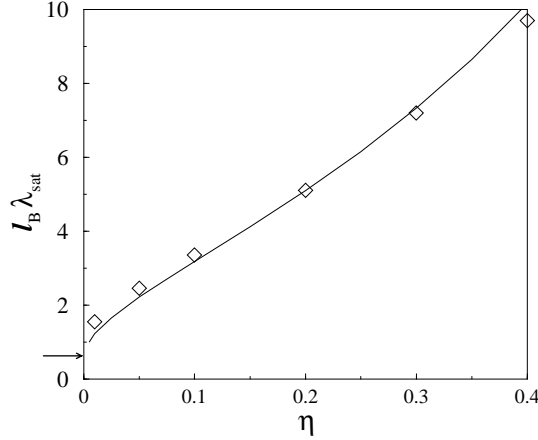


FIG. 4. Same as Fig 3 for charged rods, except that the non linear PB results are analytical here [10].

This result is compared with the effective charge deduced by applying Alexander's procedure to the analytical results of Fuoss *et al.* and Alfrey *et al.* in the large bare charge (saturation) limit [10]: the corresponding "exact" value for the effective charge is chosen such that the solution of the linearized PB equation, Eq. (32), matches the solution of the non linear PB equation (Fuoss/Alfrey *et al.* solution) at the WS boundary up to the second derivative. The resulting effective charge is plotted on Fig. 4 together with the value of the effective charge obtained within our prescription. In Fig. 5, we compare the screening factor K_{LPB} obtained within our prescription to the "exact" value K_{PB} derived from the analytical solution of the PB equation and Eq. (31) (again in the limit of a large bare charge of the cylinder where the effective charge saturates). The agreement between both quantities is remarkable, even up to extremely high packing fractions (80% on Fig. 5).

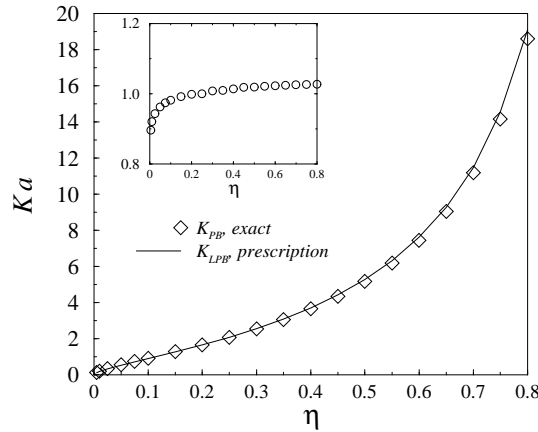


FIG. 5. Comparison of the exact inverse screening length K_{PB} obtained from the solution of PB equation (diamonds) with its counterpart K_{LPB} obtained within our prescription (continuous line), for highly charged rod-like polyions without added salt. The inset shows the ratio $K_{\text{LPB}}/K_{\text{PB}}$ as a function of packing fraction.

Another interesting check concerns the apparent potential at the surface of the cylinder. Applying again Alexander's procedure to the exact solution of Fuoss/Alfrey *et al.*, one obtains the LPB potential which matches the exact solution up to its third derivative at the WS cell boundary. The value of this potential at the surface ϕ_S^F should be compared with the value we prescribe, *i.e.* $\phi_S = 4$. The result is plotted on Fig. 6, showing again a good agreement except at low volume fraction, as expected (since as discussed in section III, our prescription is not expected to work in the very small κa limit).

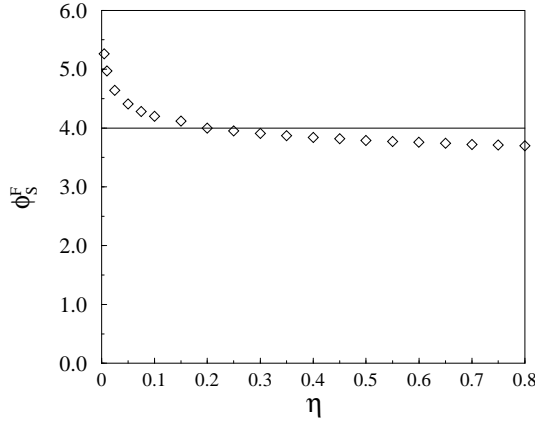


FIG. 6. Dependence on volume fraction of the reduced linearized contact potential, $\phi_S^F = \phi(a)$, with ϕ the LPB potential matching the analytical solution of the PB equation, following Alexander's procedure.

Finally, we report an intriguing result: in the limit of vanishing density it can be shown analytically that $K_{\text{PB}} R_{WS} \rightarrow \sqrt{2}$ [10]. Using this result together with $K_{\text{LPB}} a \rightarrow 0$, we obtain from Eq. (33)

$$\lim_{\eta \rightarrow 0} \lambda_{\text{sat}} = \frac{1}{\ell_B} \frac{\sqrt{2}}{2} I_1(\sqrt{2}) \simeq 0.6358 \frac{e}{\ell_B}. \quad (34)$$

This asymptotic value is displayed in Fig. 4 with an arrow. We observe that this limit is approached (although very slowly) as η decreases. Surprisingly, the result of Eq. (34) is very close to the exact expression (25) of Tracy and Widom [31] where the limit $\kappa a \rightarrow 0$ is taken after that of infinite dilution. In principle, the limits of infinite dilution and of vanishing added salt have no reason to commute. The difference between the two λ_{sat} quantities illustrates this point, with the surprise that the results are nevertheless very close numerically:

$$\lim_{\text{no salt}} \lim_{\infty \text{ dilution}} \lambda_{\text{sat}} \simeq 0.6358 \frac{1}{\ell_B} \quad (35)$$

$$\lim_{\infty \text{ dilution}} \lim_{\text{no salt}} \lambda_{\text{sat}} \simeq 0.6366 \frac{1}{\ell_B}. \quad (36)$$

V. EFFECTIVE CHARGE AT FINITE CONCENTRATION. THE FINITE IONIC STRENGTH CASE

We now turn to the case where salt is added to the colloidal suspension. More precisely, as already discussed in section II, we consider the semi grand canonical situation where the colloidal suspension is put in contact with a reservoir of salt, through a semi-permeable membrane (dialysis experiment). The concentration of mono-valent salt micro-ions in the reservoir ρ_0 fixes the chemical potential of the micro-ions in the suspension. However, due to the presence of the charged macro-ions, the salt concentration in the solution, ρ_s , differs from that in the reservoir ρ_0 : this is the so-called “salt exclusion” or “Donnan effect” [36,42,43].

As in the previous section the effect of finite concentration is accounted for within PB cell theory (using a WS sphere of radius R_{WS}). Here again, we use the prescription Eq. (26) to predict the effective charge of the macro-ions. For this purpose, it is convenient to choose that the electrostatic potential ϕ vanishes in the reservoir so that PB equation reads

$$\nabla^2 \phi = \kappa_{\text{res}}^2 \sinh \phi \quad (37)$$

where the screening factor κ_{res} is defined in terms of the ionic strength of the reservoir: $\kappa_{\text{res}}^2 = 8\pi\ell_B I_0$.

Let us now consider the linearized (“LPB”) version of this equation. We again linearize around the value of the potential at the boundary of the WS cell, $\phi_\Sigma = \phi(R_{WS})$, often referred to as the “Donnan potential”

$$\nabla^2 \delta\phi = K_{\text{LPB}}^2 (\delta\phi + \gamma_0) \quad (38)$$

where we introduced $\delta\phi = \phi - \phi_\Sigma$ and:

$$K_{\text{LPB}}^2 = \kappa_{\text{res}}^2 \cosh[\phi_{\Sigma}] \quad (39)$$

$$\gamma_0 = \tanh[\phi_{\Sigma}] = \sqrt{1 - \left(\frac{\kappa_{\text{res}}}{K_{\text{LPB}}}\right)^4}. \quad (40)$$

The second order differential equation (38) is solved invoking the two self consistent boundary conditions

$$\delta\phi = 0 \quad \text{and} \quad \frac{\partial\delta\phi}{\partial r} = 0 \quad \text{for} \quad r = R_{WS}, \quad (41)$$

so that $\delta\phi$ is known as a function of distance and depends parametrically on K_{LPB} . We emphasize that K_{LPB} is still unknown at this point. It is computed as in section IV from our prescription on the reduced potential

$$\delta\phi_S = \phi_S - \phi_{\Sigma} = 4. \quad (42)$$

A. Spheroids

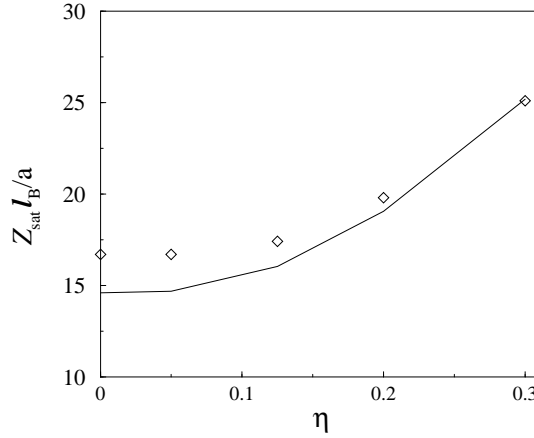


FIG. 7. Effective charge (at saturation) of spherical colloids (radius a) as a function of volume fraction η for $\kappa_{\text{res}}a = 2.6$. The continuous line is the effective charge (at saturation) computed using the prescription, while the symbols are the results of the non-linear PB cell theory, following Ref. [5].

With the same notations as above, the appropriate solution of LPB equation (38) is

$$\delta\phi_{\text{LPB}}(r) = \gamma_0 \left[-1 + f_+ \frac{e^{K_{\text{LPB}}r}}{r} + f_- \frac{e^{-K_{\text{LPB}}r}}{r} \right] \quad (43)$$

where the functions f_{\pm} are defined in Eq. (29). Note that expression (28) is recovered by taking the formal limit $\kappa_{\text{res}} = 0$ in the previous equation.

Our prescription allows to compute K_{LPB} at saturation, such that $\delta\Phi(a) = 4$, without any reference to the solution of the non linear PB problem. This equation is solved numerically using a Newton procedure. Once K_{LPB} is known, the effective charge follows from the gradient of $\delta\phi(r)$ in Eq. (43) taken at $r = a$ (it may also be computed by integrating the corresponding LPB charge density over the volume accessible to the micro-ions, i.e. $a \leq r \leq R_{WS}$)

$$Z_{\text{sat}} = \gamma_0 \frac{a}{\ell_B} \frac{1}{K_{\text{LPB}}a} \left\{ (K_{\text{LPB}}^2 a R_{WS} - 1) \sinh[K_{\text{LPB}}(R_{WS} - a)] + K_{\text{LPB}}(R_{WS} - a) \cosh[K_{\text{LPB}}(R_{WS} - a)] \right\} \quad (44)$$

with $\gamma_0 = \sqrt{1 - (\kappa_{\text{res}}/K_{\text{LPB}})^4}$. Again, our prescription $\delta\phi_S = \phi_S - \phi_{\Sigma} = 4$ provides a value for K_{LPB} which is an approximation for the exact K_{PB} at saturation, related to microions densities at the WS boundary through the expected Debye-like form

$$K_{\text{PB}}^2 = 4\pi\ell_B [\rho^+(WS) + \rho^-(WS)]. \quad (45)$$

If Eq. (44) is evaluated with the exact K_{PB} , Alexander's original effective charge follows (hence without having to implement any numerical fitting procedure). We also emphasize that as in the previous sections, the right hand side of Eq. (44) provides the effective Z_{eff} *à la* Alexander (i.e not necessarily at saturation), once evaluated with the correct K_{PB} (deduced from the numerical solution of the non-linear problem).

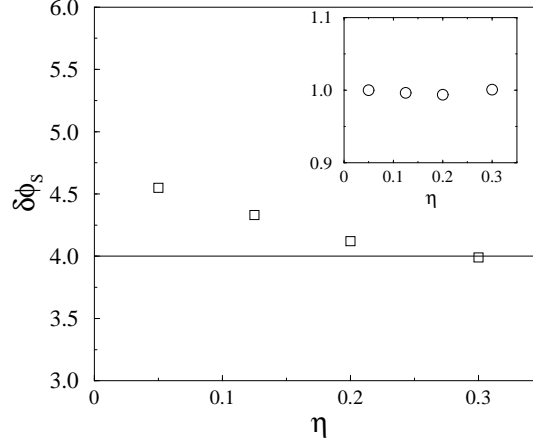


FIG. 8. Dependence on volume fraction of the “exact” reduced linearized contact potential, $\delta\phi_S = \phi(a) - \phi(R_{WS})$, with ϕ the LPB potential matched to the numerical PB solution according to Alexander’s procedure. Our prescription assumes a constant value, $\delta\phi_S = 4$. Inset: ratio $K_{\text{LPB}}/K_{\text{PB}}$ versus packing fraction. The ratio is seen to be very close to unity over the explored packing fraction window.

The results for the effective charge at saturation Z_{sat} as a function of volume fraction are displayed on Fig. 7 for $\kappa_{\text{res}}a = 2.6$. As in the previous sections, we compare this result with its Alexander’s counterpart at saturation. Our predictions are seen to be compatible with those obtained in the PB cell model.

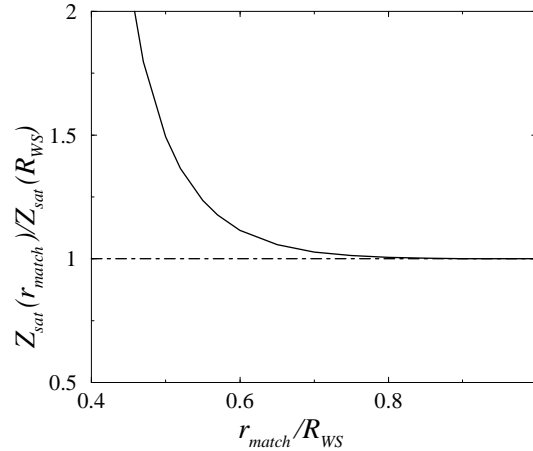


FIG. 9. Influence of the point r_{match} chosen to match the analytical LPB and numerical PB solutions on the effective charge in the saturation regime. The situation is that of a spherical polyion in a spherical WS cell, at packing fraction $\eta = 0.05$ and $\kappa_{\text{res}}a = 2.6$.

From the numerical solution of the PB equation, it is possible to extract the apparent surface potential, $\delta\phi_S = \phi(r = a) - \phi(R_{WS})$ (in the latter expression ϕ is defined as the solution of the LPB equation matching the full -numerical-PB equation up to second derivative at the WS cell boundary). By construction, this potential may be obtained inserting the numerically obtained $K_{\text{PB}} \equiv \kappa_{\text{res}} \cosh^{1/2}(\phi_S)$ into (43). This apparent potential should be compared against our prescription $\delta\phi = 4$. The corresponding result is shown on Fig. 8. We observe that $\delta\phi_S$ indeed saturates to a value close to 4. The inset shows $K_{\text{LPB}}/K_{\text{PB}}$ versus η , where K_{PB} is the “exact” screening length for the LPB equation at saturation, obtained numerically; K_{LPB} is the same quantity estimated from our prescription. We observe

that although for small packing fractions $\delta\phi_S$ slightly departs from our approximation $\mathcal{C} = 4$, the estimated K_{LPB} is still remarkably close to the exact one.

Independently of our prescription, we finally test the relevance of Alexander's procedure [5] in the following way. Z_{sat} has been obtained above from the matching of a generic LPB potential to the numerical PB one at $r_{\text{match}} = R_{WS}$. It is also possible to implement the matching at a different location inside the cell, and we denote $Z_{\text{sat}}(r_{\text{match}})$ the associated effective charge, at saturation. This quantity, normalized by the "usual" one $Z_{\text{sat}}(R_{WS})$ is displayed in Fig. 9. For the packing fraction of 5% considered, r_{match}/R_{WS} is bounded below by $a/R_{WS} \simeq 0.37$, and $Z_{\text{sat}}(R_{WS}) \simeq 16.7a/\ell_B$, see Fig. 7. We observe that Z_{sat} is relatively insensitive to r_{match} for $0.6R_{WS} \leq r_{\text{match}} \leq R_{WS}$.

B. Rod-like polyions

Using the same notations as in section IV, the appropriate solution of the LPB equation in cylindrical geometry reads

$$\delta\phi_{\text{LPB}}(\rho) = \gamma_0 \left\{ K_{\text{LPB}} R_{WS} \left[I_1(K_{\text{LPB}} R_{WS}) K_0(K_{\text{LPB}} \rho) + K_1(K_{\text{LPB}} R_{WS}) I_0(K_{\text{LPB}} \rho) \right] - 1 \right\}. \quad (46)$$

with $\gamma_0 = \sqrt{1 - (\kappa_{\text{res}}/K_{\text{LPB}})^4}$. Again, K_{LPB} is obtained as the solution of the equation $\delta\phi_{\text{LPB}}(\rho = a) = 4$. Once this equation is solved, the saturation value of the effective charge, λ_{eff} , follows from the spatial derivative of the potential $\delta\phi_{\text{LPB}}$ at the rod surface:

$$\lambda_{\text{eff}} = \frac{1}{2\ell_B} K_{\text{LPB}}^2 a R_{WS} \gamma_0 \left\{ I_1(K_{\text{LPB}} R_{WS}) K_1(K_{\text{LPB}} a) - I_1(K_{\text{LPB}} a) K_1(K_{\text{LPB}} R_{WS}) \right\}. \quad (47)$$

As in the previous sections, Eq. (47) gives analytically the relation between the effective charge *à la Alexander et al.* and micro-ions densities at the WS boundary. As such, it applies for any value of the bare charge λ , and in particular, for $\lambda \rightarrow 0$, K_{LPB} is such that $\lambda_{\text{eff}}/\lambda \rightarrow 1$. A similar remark applies for Eqs. (30), (33) and (44). If we choose for K_{LPB} the "exact" K_{PB} value, we recover the "exact" cell model (Alexander) effective charges. However, the quantity K_{LPB} solution of $\delta\phi_{\text{LPB}}(\rho = a) = 4$ is supposedly the inverse screening length at saturation and therefore provides an approximation of λ_{sat} once inserted into (47).

The corresponding results for λ_{sat} as a function of volume fraction are displayed in Fig. 10 for $\kappa_{\text{res}} a = 3$. As in the previous sections, we compare this result with its counterpart obtained from the numerical solution of PB theory together with Alexander's procedure for the effective charge in the saturation limit. The agreement with the numerical results of the full non linear PB equation is seen to be satisfactory.

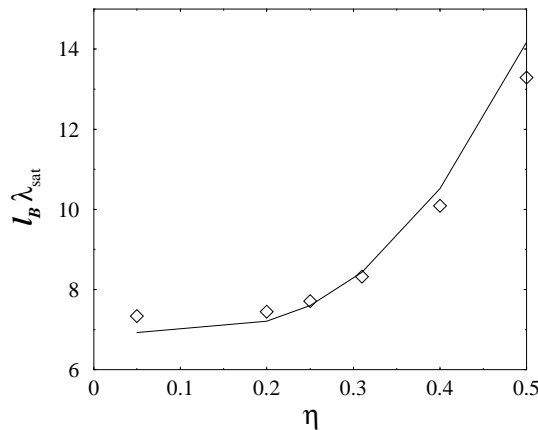


FIG. 10. Effective charge $\ell_B \lambda_{\text{sat}}$ as a function of packing fraction for cylinders with added salt ($\kappa_{\text{res}} a = 3$). The symbols represent the effective charge at saturation within the usual PB cell approach, while the continuous line follows from our prescription.

VI. CONFRONTATION TO EXPERIMENTAL AND NUMERICAL RESULTS

In the previous sections, we have tested our results for the effective charges against the numerical solutions of PB theory. However, the effective charge is a difficult quantity to measure directly in an experiment (see however the work reported in [24] confirming the scaling $Z_{\text{sat}} \propto a/\ell_B$ for low ionic strength suspensions of spherical latex colloids). In order to assess the experimental relevance of the above ideas, we now turn to the computation of osmotic properties for spherical and rod-like macro-ions, easily accessible both experimentally and within our approach. In the case of spherical colloids, we start by considering the phase behaviour of the suspension as a function of added salt.

A. Crystallization of charged spheres

The phase diagram of charged spherical colloids has been widely explored experimentally, in particular by Monovoukas and Gast [14]. In this work, the macro-ions were charged polystyrene spheres, with radius $a \simeq 660$ Å. The authors moreover compared their experimental phase diagram to that computed for particles interacting through a Yukawa potential (1) (the Yukawa phase diagram has indeed been investigated extensively by numerical simulations [44–46]). However such a comparison experiment/theory requires an ad-hoc choice for the effective charge Z_{eff} [prefactor of Eq. (1)]. The authors found that a reasonable agreement with the numerical results was obtained for a specific choice of the effective charge, $Z_{\text{sat}} = 880$ (although they reported conductimetry experiments indicating a macro-ion charge around 1200).

We focus in the following on the melting line of the phase diagram obtained in [14]. We use here our predictions for the effective charges at saturation: we do not need to know the bare charge of the polystyrene spheres, as this quantity is presumably much larger than the corresponding saturation plateau of Z_{eff} , which means, within the PB picture, that $Z_{\text{eff}} \simeq Z_{\text{sat}}$. Once Z_{sat} (and the corresponding screening constant K_{LPB} , see previous section) is known for a given density and ionic strength, it is possible to insert it into the computed generic phase diagram of Yukawa systems [44] to obtain the corresponding stable phase. We extract in particular the melting line from these numerical results: we prefer to use these numerical results for the phase diagram (instead of performing a full theoretical analysis) since our main focus remains to check the relevance of our predictions for the effective charges. This requires a “reliable” description for the melting line, which numerical simulations provide once the potential is given.

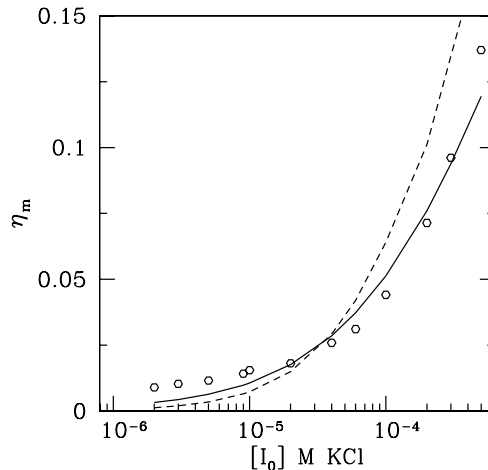


FIG. 11. Liquid-solid transition of charged polystyrene colloids: volume fraction for melting η_m as a function of salt ionic strength I_0 . Dots are experimental points for the melting line extracted from Ref. [14]. The solid line is the theoretical prediction for the melting transition using our prescription for effective charges (see text) while the dashed line corresponds to an ad hoc fixed effective charge $Z_{\text{eff}} = 880$, as proposed in [14].

We emphasize that at this level, the only parameter entering our description is the diameter of the beads, which is measured independently. Accordingly, there is *no adjustable parameter* in our equations and the resulting phase diagram is strongly constrained. The results for the melting line using our prescription for the effective charge are confronted to the experimental data in Fig. 11. We also plot the result for the melting line for an ad hoc constant

effective charge, $Z_{\text{sat}} = 880$, as was proposed in Ref. [14]. The observed agreement supports the pertinence of our prescription for Z_{sat} which reproduces the experimental phase diagram. In our case, the effective charge does vary between 500 and 2000 along the melting line, depending on ionic strength and density. This could explain that the conductimetry measurements performed independently by Monovoukas and Gast (although at an unspecified ionic strength) yield another value for the effective charge of the spheres ($Z \sim 1200$ as quoted above).

B. Osmotic pressure of a suspension of spherical colloids

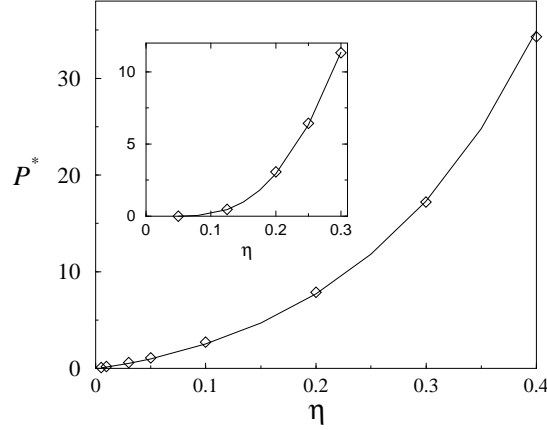


FIG. 12. Reduced osmotic pressure $P^* = 4\pi\ell_B a^2 \Pi_{\text{osm}}/kT$ versus volume fraction for spherical polyions in the salt free case where I_0 (and thus κ_{res}) vanishes. The symbols are the PB values obtained from the resolution of the non-linear problem, and the line follows from our prescription. The inset shows the same quantities in presence of an electrolyte ($\kappa_{\text{res}} a = 2.6$).

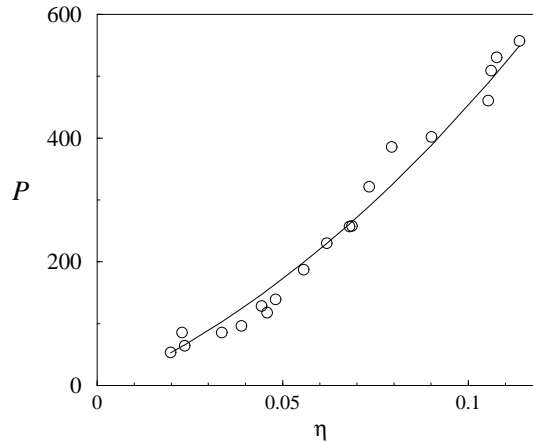


FIG. 13. Osmotic pressure (in Pa) as a function of volume fraction. The symbols are the experimental measures of [49] for aqueous suspensions of bromopolystyrene particles (with radius $a = 51$ nm). The continuous curve corresponds to our prescription assuming a salt concentration of 10^{-6} M in the reservoir.

In the PB cell model, the osmotic pressure in the solution is related to the densities of micro-ions at the WS cell boundary [7,36,47,48]:

$$\Pi_{\text{osm}} = k_B T [\rho^+(R_{WS}) + \rho^-(R_{WS}) - 2\rho_0], \quad (48)$$

where we have subtracted the ionic contribution from the reservoir (of salt density $\rho_0 = I_0$). This is because the electric field vanishes at the WS cell and there is no contribution from the electrostatic pressure at $r = R_{WS}$. Using Eq. (45), Eq. (48) may be recast into

$$\Pi_{\text{osm}} = \frac{k_B T}{4\pi\ell_B} [K_{\text{PB}}^2 (\rho, I_0) - \kappa_{\text{res}}^2], \quad (49)$$

where κ_{res} is the screening constant defined in terms of the ionic strength in the reservoir. Our prescription is supposed to give an excellent approximate of the non-linear K_{PB} through K_{LPB} , and readily allows an estimation of the osmotic pressure. Figure 12 shows the accuracy of the estimate, with or without added electrolyte.

The comparison of our predictions *at saturation* to the experimental results reported by Reus *et al.* [49] is also satisfactory, see Fig. 13. It was already pointed out in [49] that PB cell theory reproduced well the experimental data. The agreement observed in Fig. 13 however illustrates the relevance of the PB saturation picture –well captured by our approach– at high polyion/micro-ion electrostatic coupling (see the discussion in section VII).

C. Osmotic properties of rod-like polyions

Expression (49) is also valid in cylindrical geometry, and we show in Fig. 14 the comparison prescription versus non-linear PB osmotic pressure. We draw a similar conclusion as for spherical polyions concerning the accuracy of our approximation.

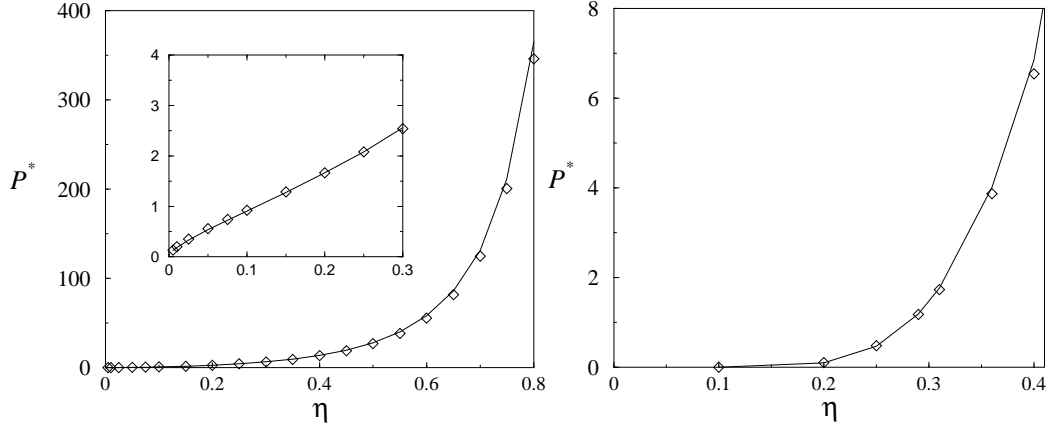


FIG. 14. Same as Fig. 12 for cylindrical polyions. Top: salt free suspensions (the inset is a zoom in the small packing fraction region). Bottom: situation with added salt ($\kappa a = 3$).

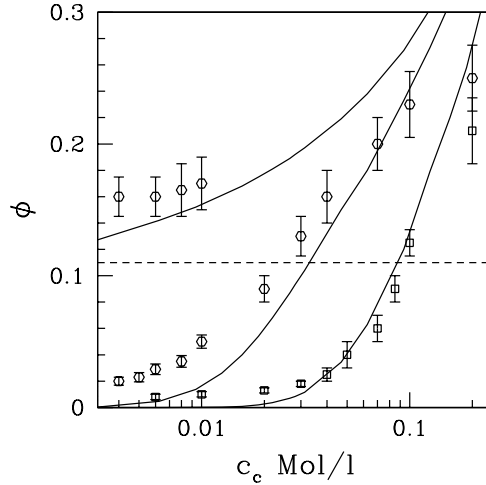


FIG. 15. Osmotic coefficient ϕ of B-DNA solutions as a function of density of DNA phosphate ions c_c , for ionic strengths of 10 mM, 2mM and 0 mM (from bottom to top). The dots are the experimental points obtained from Refs. [50,51], while the solid lines correspond to the predictions for ϕ using our prescription in cylindrical geometry. The dashed line is the prediction of Oosawa-Manning condensation theory.

For completeness, we compare in what follows our estimate for the osmotic pressure to the experimental results on B-DNA solutions reported in [50,51]. In this work, the authors measured the osmotic coefficient $\phi = \Pi_{\text{osm}}/\Pi_c$, defined as the ratio between the osmotic pressure Π_{osm} to the pressure Π_c of releasable counter-ions having bare density c_c ($\Pi_c = k_B T c_c$) against the concentration of B-DNA, a rigid cylindrical polyelectrolyte. A related PB cell analysis may be found in [48] while a more thorough investigation has been performed in [52].

Within the WS model, B-DNA macro-ions are confined into cylindrical cells, which radius R_{WS} is related to the bare concentration of DNA counter-ions as $c_c = (\ell_{DNA} \pi R_{WS}^2)^{-1}$, with $\ell_{DNA} = 1.7 \text{ \AA}$ the distance between charges along DNA. Note that as in the previous section dealing with charged spheres, there is no adjustable parameter in our description since the radius of the DNA and the bare charge (only used to normalize the osmotic pressure to Π_c) are known from independent measurements. In Fig. 15, the corresponding results for the osmotic coefficient are confronted against the experimental data of Refs. [50,51] for various ionic strengths, showing again a good quantitative agreement. As in Ref. [7], we report the prediction of classical Oosawa-Manning condensation theory (see e.g. [19,52]), for which the osmotic coefficient is constant [$\phi = \ell_{DNA}/(2\ell_B)$] at complete variance with the experiments. In view of the results reported in Fig. 14, the disagreement at small c_c may be attributed to the (relative) failure of PB theory, and not to a weakness of our prescription that should be judged with respect to non-linear PB.

VII. DISCUSSION - VALIDITY OF THE APPROACH

Our analysis was carried out at the level of Poisson-Boltzmann theory, which is mean-field like. More refined approaches such as the salt free Monte Carlo simulations of Groot [53] for the cell model within the primitive model [54] have shown a non-monotonic behaviour of Z_{eff} upon increasing Z for spheres: after the linear regime where $Z_{\text{eff}} \simeq Z$, Z_{eff} reaches a maximum for a value Z_{bare}^* and then decreases. When the radius a of the charged spheres is much larger than Bjerrum length ℓ_B , this maximum is surrounded by a large plateau in excellent agreement with the PB saturation value Z_{sat} [15,53]. PB theory appears to become exact for $\ell_B/a \rightarrow 0$ [55]. Given that, Z_{bare}^* scales like $(a/\ell_B)^2$ and therefore becomes quickly large when the colloid size is increased [53], PB theory is successful in the colloidal limit of large a . We recall that this is precisely the limit where our predictions for the effective charge at saturation Z_{sat} are reliable (the condition $a \gg \kappa^{-1}$ should *a priori* be satisfied even if we have shown above that our predictions remain fairly accurate down to κa of order 1). More generally, the results of Groot [53] show that the effective charge Z_{eff} from Monte Carlo simulations within the primitive model for arbitrary a/ℓ_B are smaller than the quantity Z_{sat} of PB theory. This is a general feature that neglect of ionic correlation (as in PB) leads to an underestimated screening of the macro-ion by the micro-ions, and thus to overestimated effective charges (see e.g. [52,56] in cylindrical geometry). Our approach thus provides a useful upper limit for a realistic Z_{eff} .

A related comment in favor of the validity of PB picture with a saturation plateau for Z_{eff} comes from the work of Cornu and Jancovici [57]. For the two dimensional two-component Coulomb gas bounded by a hard wall of surface charge σ , these authors performed an exact calculation at the inverse reduced temperature $e^2/(kT) = 2$ showing that the effective surface charge of the wall saturates to a plateau value when σ diverges.

Generally speaking, in an 1:1 electrolyte, PB theory seems to be a reasonable approximation [58,59], all the better that the size of the macro-ion is larger than ℓ_B ; the notion of charge renormalization then encapsulates the main effects of the non-linear PB theory, and is consistent with experimental data on dilute bulk solution [60,61] (see also the experimental work cited in section VI). For micro-ions of higher valences (di- or tri-valent), strong ionic correlations rule out PB-like approaches, as shown by recent computer simulations of the primitive model [62–64]. As a consequence, the results presented here should *a priori* not be used in the interpretation of experiments involving multivalent salts or counter-ions. For a discussion concerning the effects of multivalent counter-ions, we refer to the review by Bhuiyan, Vlachy and Outhwaite [65].

VIII. CONCLUSION

The notion of effective charge is widely used in the fields of colloidal suspensions. It allows in practice to describe the phase behavior of (highly) charged macro-ions staying at the level of linearized Poisson-Boltzmann equations, where the macro-ions are supposed to interact through Yukawa-like pair potentials. However, no general analytical description of this renormalization process is available and the effective charge is usually left as a free parameter, adjusted to fit experimental (or numerical) data. Physically the charge renormalization process results from the strong coupling of the micro-ions in the vicinity of the highly charged colloidal particle. At the level of Poisson-Boltzmann theory, the effective charge saturates to a finite value in the limit where the bare charge becomes large.

We recall that omission of the non-linearities of PB theory –correctly accounted for by the notion of effective charge– may lead to unphysical results (see e.g. [36,66]).

In the present paper, we have put forward a simple method to estimate the effective charge of highly charged colloidal objects either analytically, or through the resolution of a simple equation obtained within linearized Poisson-Boltzmann approximation. This approach (mostly suited to describe the colloidal limit $\kappa a \gg 1$) amounts to consider the highly charged colloids as objects with constant electrostatic potential $\sim 4kT/e$, independently of shape and physico-chemical parameters (size, added 1:1 electrolyte...). This result relies on the physical picture that the electrostatic energy eV_0 of the strongly coupled micro-ions (*i.e.* micro-ions in the vicinity of the highly charged macro-ion) does balance their thermal (entropic) energy $k_B T$, resulting in a constant effective surface potential for the “dressed” macro-ion. We have successfully tested this approach against *a)* the geometry of the solid particle, *b)* the confinement (finite concentration situations), *c)* the presence of added salt, *d)* exact and approximate solutions of the full non-linear PB equations *e)* direct experimental measurements of the effective charge found in the literature. From these different checks, we conclude that our prescription appears to contain the key ingredients involved in charge renormalization.

An important point is that the effective charge is not constant and depends explicitly on the physical conditions of the experiment, through ionic strength, density, etc The effect is quite obvious in the small dilution limit, where we found that the (saturated) effective charge is an *increasing* function of κ (for $\kappa a > 1$, which stems from the reduction of the attraction between the counter-ions and the colloid. It pertains for finite concentration and the effective charge increases with the ionic strength in the suspension. Addition of salt consequently brings two antagonist effects on the effective Coulombic interaction between macro-ions: the range of the interaction decreases due to screening, while the amplitude increases due to the effective charge. The competition between these two effects might be a key point in the understanding of these systems. It appears therefore interesting to reconsider the phase stability of macro-ion suspension in light of these results (see also [68] and more recently [69]).

Eventually it would be desirable to extend our approach to the case of finite size colloidal particles, such as rods with finite length or disks [47]. Accordingly, edge effects should show up at the level of our prescription and result in an effective charge distribution along the macro-ion, due to the constant potential prescription on the object. Work along these lines is in progress.

Acknowledgments: We would like to thank J.P. Hansen, H. Löwen, H.H. von Grünberg, M. Deserno, C. Holmand, J.F. Joanny for useful discussions.

-
- [1] E.J.W. Verwey and J.T.G. Overbeek, *Theory of the Stability of Lyophobic Colloids*, Elsevier, Amsterdam, 1948.
 - [2] R. Kjellander and D.J. Mitchell, Chem. Phys. Lett. **200**, 76 (1992).
 - [3] J. Ulander, H. Greberg, and R. Kjellander, J. Chem. Phys. **115**, 7144 (2001) and references therein.
 - [4] L. Belloni, Colloids Surfaces A: Physicochem. Eng. Aspects **140**, 227 (1998).
 - [5] S. Alexander, P.M. Chaikin, P. Grant, G.J. Morales and P. Pincus, J. Chem. Phys. **80**, 5776 (1984).
 - [6] R.J. Hunter, *Foundations of Colloid Science*, (Clarendon, Oxford, 1995).
 - [7] J.-P. Hansen and H. Löwen, Annu. Rev. Phys. Chem. **51**, 209 (2000).
 - [8] This terminology should be used remembering that except in cylindrical geometry, there is no *physical* condensation (defined as the existence of a non vanishing quantity of micro-ions in a layer of vanishing thickness around the polyion, see references [9–11]).
 - [9] J.-L. Barrat and J.-F. Joanny, Adv. Chem. Phys. **94**, 1 (1996).
 - [10] R.M. Fuoss, A. Katchalsky and S. Lifson, Proc. Natl. Acad. Sci. U.S.A. **37**, 579 (1951); T. Alfrey, P. Berg and H.J. Morawetz, J. Polym. Sci. **7**, 543 (1951).
 - [11] G.V. Ramanathan, J. Chem. Phys. **78**, 3223 (1983).
 - [12] P. Attard, Adv. Chem. Phys. **92**, 1 (1996).
 - [13] C.N. Likos, Physics Reports **348**, 267 (2001).
 - [14] Y. Monovoukas and A. P. Gast, J. Colloid and Interf. Sci. **128**, 533 (1989).
 - [15] M.J. Stevens, M.L. Falk and M.O. Robbins, J. Chem. Phys. **104**, 5209 (1996).
 - [16] In this respect, it is important to realize that for an infinitely long rod in the Manning limit, the effective line charge λ_{eff} is smaller than the equivalent charge λ_{equiv} . For large bare charges, we have in particular $\lambda_{\text{sat}} < 1/\ell_B$, see the discussion in section III.
 - [17] A. Diehl, M.C. Barbosa and Y. Levin, Europhys. Lett. **53**, 86 (2001).
 - [18] P.S. Kuhn, Y. Levin and M.C. Barbosa, Macromolecules **31**, 8347 (1998).
 - [19] M. Deserno, C. Holm and S. May, Macromolecules **33**, 199 (2000).

- [20] L. Belloni, J. Phys.: Condens. Matter **12**, R549 (2000).
- [21] E. Trizac, L. Bocquet and M. Aubouy, to appear in Physical Review Letters and cond-mat/0201510.
- [22] E. Trizac, Phys. Rev. E **62**, R1465 (2000).
- [23] I.A. Shkel, O.V. Tsodirov and M.T. Record, J. Phys. Chem. B, **104**, 5161 (2000).
- [24] P. Wette, H.J. Shöpe and T. Palberg, J. Chem. Phys. **116**, 10981 (2002).
- [25] J.C. Crocker and D.G. Grier, Phys. Rev. Lett. **77**, 1897 (1996).
- [26] S.H. Behrens and D.G. Grier, J. Chem. Phys. **115**, 6716 (2001).
- [27] H. Oshima, T. Healy and L.R. White, J. Colloid Interface Sci. **90**, 17 (1982).
- [28] G.V. Ramanathan, J. Chem. Phys. **88**, 3887 (1988).
- [29] T.M. Squires and M.P. Brenner, Phys. Rev. Lett. **81**, 4976 (2000).
- [30] A.M. Larsen and D.G. Grier, Nature **385**, 230 (1997).
- [31] C.A. Tracy and H. Widom, Physica A **244**, 402 (1997).
- [32] M. Fixman, J. Chem. Phys. **70**, 4995 (1979).
- [33] R.A. Marcus, J. Chem. Phys. **23**, 1057 (1955).
- [34] E. Trizac and J.-P. Hansen, J. Phys.: Condens. Matt. **8**, 9191 (1996).
- [35] M. Deserno and C. Holm in: Proceedings of the NATO Advanced Study Institute on Electrostatic Effects in Soft Matter and Biophysics, ed. by C. Holm et al., Kluwer (2001).
- [36] M. Deserno and H.H. von Grünberg, Phys. Rev. E **66**, 011401 (2002).
- [37] W. Härtl and H. Versmold, J. Chem. Phys. **88**, 7157 (1988).
- [38] H. Löwen, J. Chem. Phys. **100**, 6738 (1994).
- [39] V. Lobaskin and P. Linse, J. Chem. Phys. **111**, 4300 (1999).
- [40] E. Allahyarov and H. Löwen, J. Phys.: Condens. Matt. **13**, L277 (2001).
- [41] A.G. Moreira and R.R. Netz, Phys. Rev. Lett. **87**, 078301 (2001); R.R. Netz, Eur. Phys. J. E **5**, 557 (2001).
- [42] M. Dubois, T. Zemb, L. Belloni, A. Delville, P. Levitz and R. Setton, J. Chem. Phys. **75**, 944 (1992).
- [43] J.P. Hansen and E. Trizac, Physica A **235**, 257 (1997).
- [44] M.O. Robbins, K. Kremer, G.S. Grest, J. Chem. Phys. **88** 3286 (1988).
- [45] E.J. Meijer and D. Frenkel, J. Chem. Phys. **94**, 2269 (1991).
- [46] F. Bitzer, T. Palberg, H. Löwen, R. Simon and P. Leiderer, Phys. Rev. E **50**, 2821 (1994).
- [47] E. Trizac and J.-P. Hansen, Phys. Rev. E **56**, 3137 (1997).
- [48] P.L. Hansen, R. Podgornik, and V.A. Parsegian, Phys. Rev. E **64**, 021907 (2001).
- [49] V. Reus, L. Belloni, T. Zemb, N. Lutterbach and H. Versmold, J. Phys. II France **7**, 603 (1997).
- [50] H.E. Auer and Z. Alexandrowicz, Biopolymers **8**, 1 (1969).
- [51] E. Raspaud, L. da Conceicao, and F. Livolant, Phys. Rev. Lett. **84**, 2533 (2000).
- [52] M. Deserno, C. Holm, J. Blaul, M. Ballauff, M. Rehahn, Eur. Phys. J. E **5**, 97 (2001).
- [53] R.D. Groot, J. Chem. Phys. **95**, 9191 (1991).
- [54] which neglects the discrete nature of the solvent, but takes into account the micro-ions explicitly as hard bodies.
- [55] with the mathematical restriction that $Z\ell_B/a$ remains finite.
- [56] M. Deserno and C. Holm, cond-mat/0203599.
- [57] F. Cornu and B. Jancovici, J. Chem. Phys. **90**, 2444 (1989).
- [58] B. Hribar, V. Vlachy V, L.B. Bhuiyan and C.W. Outhwaite, J. Phys. Chem B **104**, 11533 (2000).
- [59] A. Evilevitch, V. Lobaskin, U. Olsson, P. Linse and P. Schurtenberger, Langmuir **17**, 1043 (2001).
- [60] T. Palberg, W. Mönch, F. Bitzer, R. Piazza and T. Bellini, Phys. Rev. Lett. **74**, 4555 (1995).
- [61] J.C. Crocker and D.G. Grier, Phys. Rev. Lett. **73**, 352 (1994).
- [62] E. Allahyarov, I. d'Amico and H. Löwen, Phys. Rev. Lett. **81**, 1334 (1998).
- [63] P. Linse and V. Lobaskin, Phys. Rev. Lett. **83**, 4208 (1999).
- [64] R. Messina, C. Holm and K. Kremer, Phys. Rev. Lett. **85**, 872 (2000).
- [65] L.B. Bhuiyan, V. Vlachy and C.W. Outhwaite, Int. Reviews in Physical Chemistry **21**, 1 (2002).
- [66] H.H. von Grünberg, R. van Roij and G. Klein, Europhys. Lett **55**, 580 (2001).
- [67] See e.g. D. Andelman in *Membranes, their Structure and Conformation*, edited by R. Lipowsky and E. Sackmann (Elsevier, Amsterdam 1996).
- [68] B. Beresford-Smith, D.Y.C. Chan and D.J. Mitchell, J. Colloid Interface Sci. **216** 9691 (1985).
- [69] L.F. Rojas, C. Urban, P. Schurtenberger, T. Gisler and H.H. von Grünberg, submitted to Europhysics Letters.

APPENDIX A: ANALYTICAL SOLUTION OF PB EQUATION FOR AN ISOLATED PLANE IN AN ELECTROLYTE

Here, we recall the analytical solution of PB equation for an isolated plane of bare surface charge σe immersed in an electrolyte of bulk ionic strength I_0 . In this case, the solution of equation (6) reads [67]:

$$\phi_{\text{PB}}(z) = 2 \ln \frac{1 + \gamma e^{-\kappa z}}{1 - \gamma e^{-\kappa z}} \quad (\text{A1})$$

where $\gamma = \sqrt{x^2 + 1} - x$, $\kappa^2 = 8\pi\ell_B I_0$ and $x = \kappa\lambda_{GC}$, with the Gouy-Chapman length defined as

$$\lambda_{GC} = \frac{1}{2\pi l_B \sigma}. \quad (\text{A2})$$

Far from the charged surface, say $z > 2\kappa^{-1}$, the solution of PB equation reduces to

$$\phi_{\text{PB}}(z) \simeq \phi_S e^{-\kappa z} \quad (\text{A3})$$

with $\phi_S = 4\gamma$. The potential ϕ_S can be interpreted as the *apparent* reduced potential extrapolated at contact. In the following we shall simply refer to ϕ_S as the *apparent potential*.

As expected, this asymptotic expression for the reduced potential ϕ_{PB} in Eq. (A3) precisely matches the solution ϕ_{LPB} of the linearized PB (LPB) equation:

$$\nabla^2 \phi_{\text{LPB}} = \kappa^2 \phi_{\text{LPB}} \quad (\text{A4})$$

but with the fixed charge boundary condition on the plane replaced by an effective *fixed surface potential* boundary condition $\phi_{\text{LPB}}(z=0) = \phi_S = 4\gamma$. The effective charge density is then computed using Gauss theorem at the surface, yielding

$$\sigma_{\text{eff}} = \frac{\gamma\kappa}{\pi l_B}. \quad (\text{A5})$$

In doing so, we have replaced the initial non linear PB equation with fixed charge boundary condition by the linear LPB equation with fixed surface potential.

Now at fixed κ (*i.e.* constant ionic strength), we progressively increase the bare surface charge σ . Accordingly $\kappa\lambda_{GC} \rightarrow 0$ and the parameter γ goes to 1. From Eq. (A5), we obtain that the effective charge and the apparent potential ϕ_S have a simple behaviour depending on the comparison of σ with σ_{sat} defined as

$$\sigma_{\text{sat}} = \frac{\kappa}{\pi l_B}. \quad (\text{A6})$$

Indeed

$$\begin{aligned} \sigma \ll \sigma_{\text{sat}} \quad & \sigma_{\text{eff}} \cong \sigma \\ & \phi_S \cong 4\sigma/\sigma_{\text{sat}} \end{aligned} \quad (\text{A7})$$

$$\begin{aligned} \sigma \gg \sigma_{\text{sat}} \quad & \sigma_{\text{eff}} \cong \sigma_{\text{sat}} \\ & \phi_S \cong 4 \end{aligned} \quad (\text{A8})$$

The important point is that in the large bare charge limit, $\sigma \gg \sigma_{\text{sat}}$, the effective charge σ_{eff} saturates to a value σ_{sat} independent of the bare one, σ . In this limit, the apparent potential also saturate to a constant value, $\phi_S = 4$.

APPENDIX B: ANALYTICAL SOLUTION OF PB EQUATION FOR A CONFINED PLANE WITHOUT ADDED SALT

An infinite plane (bare surface charge density σe) is placed in the middle of a Wigner-Seitz slab of width $2h$. The origin of coordinates $x = 0$ is chosen at the location of the plane such that the volume available to the counter-ions is $-h \leq x \leq h$. For symmetry reasons, it is enough to solve the problem for $x > 0$. The electrostatic potential ϕ obeys PB equation (4), supplemented with Neumann boundary conditions: $\nabla\phi(h) = 0$, corresponding to the electroneutrality

condition; $\nabla\phi(0) = -2\pi\ell_B\sigma$ imposing the charge on the plane. Without loss of generality, we choose the origin of potential such that $\phi(h) = 0$; the analytical solution of PB equation then reads [67]

$$\phi_{\text{PB}}(x) = -\log \left[\cos^2 \left(\frac{(|x| - h)}{\sqrt{2}K_{\text{PB}}^{-1}} \right) \right], \quad (\text{B1})$$

where $K_{\text{PB}}(\sigma)$ is such that

$$\frac{hK_{\text{PB}}}{\sqrt{2}} \tan \left(\frac{hK_{\text{PB}}}{\sqrt{2}} \right) = \pi\ell_B\sigma h. \quad (\text{B2})$$

The inverse screening length K_{PB} is related to the density of counter-ions at the WS boundary $\rho^-(h)$ through the following expression, reminiscent of the standard definition of the Debye length

$$K_{\text{PB}}^2 = 4\pi\ell_B\rho^-(h). \quad (\text{B3})$$

Now we consider the corresponding LPB equation. More precisely, we linearize Eq. (4) around $x = h$ (*i.e.* the edge of the slab). Since we have chosen $\phi_{\text{PB}}(h) = 0$, we impose ϕ_{LPB} to vanish at $x = h$. The resulting equation reads

$$\nabla^2\phi = K_{\text{LPB}}^2(\phi + 1) \quad (\text{B4})$$

where we have introduced K_{LPB} , an “apparent” local Debye screening factor for the linearized PB equation. As for the previous PB equation in the no salt case, K_{LPB} is not known *a priori* but results from the electroneutrality condition. Indeed, solving Eq. (B4) with the appropriate boundary conditions [$\nabla\phi(h) = 0$, $\nabla\phi(0) = 4\pi\ell_B(\sigma/2)$] yields

$$\phi_{\text{LPB}}(x) = \cosh [K_{\text{LPB}}(x - h)] - 1, \quad (\text{B5})$$

with $K_{\text{LPB}}(\sigma)$ such that

$$hK_{\text{LPB}} \sinh [K_{\text{LPB}}h] = 2\pi\ell_B\sigma h \quad (\text{B6})$$

Note that comparing Eqs. (B2) and (B6), we see that $K_{\text{LPB}}(\sigma) \neq K_{\text{PB}}(\sigma)$. It is however crucial to remember that the LPB solution should not be used with the bare charge σ to describe the correct behaviour of ϕ_{PB} in the vicinity of $x = h$.

Next, we implement the procedure proposed by Alexander to find the effective charge in confined situations [5]. The effective charge density is accordingly the value of σ in the linearized PB equation such that $\phi_{\text{PB}}(x)$ and $\phi_{\text{LPB}}(x)$ match up to the second derivative at Σ , the boundary of the WS cell [5]. This condition is equivalent to set

$$K_{\text{LPB}}(\sigma_{\text{eff}}) = K_{\text{PB}}(\sigma). \quad (\text{B7})$$

Note that in general, whenever the solution of the non-linear PB problem is known, the effective charge σ_{eff} can be directly estimated with Eq. (B7) (this is of course quite academic to obtain in this case an effective charge since the full solution for the potential is known; the notion of effective charge is mostly useful in geometries where no analytical solution of the PB equation is known). Note also that whenever Eq. (B7) is verified, the third, fourth and fifth derivative of the linear and non-linear solutions also match at Σ .

One deduces eventually the “exact” effective charge from Eq. (B7) for the plane case (by “exact” we mean that the effective charge is obtained from the analytical solution of PB equation, in contrast to our prescription):

$$\sigma_{\text{eff}} = \frac{K_{\text{PB}}(\sigma) \sinh [K_{\text{PB}}(\sigma)h]}{2\pi\ell_B}. \quad (\text{B8})$$

The apparent potential ϕ_S is also obtained as

$$\phi_S = \phi_{\text{LPB}}(0) = \cosh [K_{\text{PB}}(\sigma)h] - 1. \quad (\text{B9})$$

From Eq. (B2), we define a critical value for the charge density

$$\sigma_c = \frac{1}{\pi\ell_B h} \quad (\text{B10})$$

and we find the asymptotic behaviors

$$\sigma \ll \sigma_c \quad \left\{ \begin{array}{l} hK_{\text{PB}} \cong (2\sigma/\sigma_c)^{1/2} \\ \sigma_{\text{eff}} \cong \sigma \\ \phi_S \cong 2\sigma/\sigma_c \end{array} \right. \quad (\text{B11})$$

$$\sigma \gg \sigma_c \quad \left\{ \begin{array}{l} hK_{\text{PB}} \cong \pi/\sqrt{2} \\ \sigma_{\text{eff}} \cong \sigma_{\text{sat}} = \frac{\pi}{2\sqrt{2}} \sinh \left[\frac{\pi}{\sqrt{2}} \right] \sigma_c \cong 5.06\sigma_c \\ \phi_S \cong \cosh \left[\frac{\pi}{\sqrt{2}} \right] - 1 \cong 3.66 \end{array} \right. \quad (\text{B12})$$

As in the infinite dilution limit, one obtains that the effective charge σ_{eff} coincides with the bare one σ for small σ , and saturates to a finite value when $\sigma \rightarrow \infty$. However both σ_c and the saturation value for the effective charge at finite concentration differ from the σ_{sat} of infinite dilution [Eq. (A6)]. We also note that strictly speaking, the limits of infinite dilution and of vanishing added salt do not commute: if the limit of vanishing salt is taken first (situation investigated in this appendix), before $h \rightarrow \infty$, we obtain $\phi_S^{\text{sat}} = \cosh [\pi/\sqrt{2}] - 1$, whereas reverting the order corresponds to the planar situation of Appendix A with $\kappa \rightarrow 0$, and there, we have $\phi_S^{\text{sat}} = 4$. In both cases however, the effective charge at saturation vanishes.